

Sensitivity of L-Band Radar Backscatter to Forest Biomass in Semiarid Environments: A Comparative Analysis of Parametric and Nonparametric Models

Mihai A. Tanase, Rocco Panciera, Kim Lowell, Siyuan Tian, Alberto García-Martín, and Jeffrey P. Walker

Abstract—This paper investigated the effectiveness of frequently used parametric and nonparametric models for biomass retrieval from L-band radar backscatter. Two areas, one in Spain and one in Australia, characterized by different tree species, forest structure, and field sampling designs were selected to demonstrate that retrieval error metrics are similar for different local conditions and sampling characteristics. A mixed-model retrieval strategy was proposed to reduce the overall (i.e., across the entire biomass range) as well as by-biomass-interval errors. Significant relationships were found between aboveground biomass and radar backscatter with most of the backscatter dynamic range being limited to a fairly low range of biomass values (< 30 t/ha) in both study areas. Biomass retrieval errors were largely similar for all parametric and nonparametric models tested. However, some parametric models consistently provided lower correlation between the observed and the predicted biomass while nonparametric models generally provided an unbiased estimation. A mixed-model retrieval strategy was shown to reduce biomass estimation errors by up to 15%. Biomass retrieval errors were highly variable within the L-band sensitivity interval, suggesting that overall accuracy estimates should be used with care, particularly for low biomass intervals (< 30 t/ha) where surface scattering could dominate the total backscatter. Despite exhibiting the highest dynamic range, low biomass areas were characterized by the highest estimation errors (in excess of 80%). Conversely, relative estimation errors were as low as 20%–35% for the 30–75 t/ha biomass intervals, while at higher biomass levels, the estimation error increased due to signal saturation.

Index Terms—ALOS PALSAR, backscatter, forest biomass, L-band, parametric and non-parametric modeling.

I. INTRODUCTION

THE retrieval of forest characteristics is currently one of the main research topics of the remote sensing community with the accurate estimation of carbon emissions from deforestation and forest degradation being a major challenge.

Manuscript received February 20, 2013; revised May 26, 2013 and August 10, 2013; accepted September 10, 2013. This work was supported in part by the Australian Research Council (ARC) Superscience Fellowship under Grant FS100100040 and in part by the Cooperative Research Centre for Spatial Information.

M. A. Tanase, R. Panciera, K. Lowell, and S. Tian are with the Cooperative Research Centre for Spatial Information, The University of Melbourne, Carlton, Vic. 3053, Australia.

A. García-Martín is with the Department of Geography, The University of Zaragoza, Zaragoza 50009, Spain.

J. P. Walker is with the Department of Civil Engineering, Monash University, Clayton, Vic. 3800, Australia.

Color versions of one or more of the figures in this paper are available online at <http://ieeexplore.ieee.org>.

Digital Object Identifier 10.1109/TGRS.2013.2283521

Forest carbon stock estimation is a sensitive research topic since information on forest spatial distribution, biomass levels, and dynamics is needed for greenhouse gases flux estimation and, thus, policy development and implementation [1].

The last two decades have been strongly focused on the extraction of biomass estimates from synthetic aperture radar (SAR) sensors after relationships between forest biomass and radar backscatter coefficients were demonstrated more than three decades ago [2]. Global coverage, high temporal and spatial resolutions, and independence from cloud cover were the main attractive features of spaceborne SAR sensors. The sensitivity of SAR backscatter to biomass levels depends mostly on system wavelength, with P-band (around 64-cm wavelength) recognized early on as the most sensitive due to its greater penetration of the vegetation [3]–[6]. However, most recent research was focused on L-band due to the availability of such data from the Japanese Earth Resources Satellite (JERS) and Advanced Land Observing Satellite (ALOS) Phased Array type L-band Synthetic Aperture Radar (PALSAR). The potential for using L-band radar backscatter to estimate aboveground biomass (AGB) has been studied for most forest types, ranging from boreal to tropical regions using airborne and/or spaceborne sensors [6]–[14]. The consensus among such studies is that backscatter coefficients increase with biomass until a saturation point is reached which is influenced by forest type/structure and environmental conditions (i.e., rainfall, freeze/thaw cycles, etc.) as well as sensor characteristics such as wavelength and polarization. The observed saturation point is usually between 30 and 100 t/ha across most forest types and radar polarizations [3], [5], [9], [15]. Previous studies also showed that L-band cross-polarized radar backscatter was more sensitive to variations in biomass [3], [16], [17], whereas copolarized backscatter showed greater sensitivity to differences in forest cover fraction. The dynamic range (i.e., the difference between maximum and minimum backscatter values recorded for different vegetation densities) has been seen to vary between 4 and 10 dB for L-band cross-polarized data [11], [17]. Most of this dynamic range, however, covers only a relatively small biomass span, usually below 50 t/ha. For the remaining biomass range up to the saturation point, the backscatter increase is modest, frequently within 2–3 dB, which could hinder retrieval algorithms [9], [11], [15], [18]–[21]. A number of biomass retrieval strategies have emerged, the majority of which were based on parametric (i.e., empirical and semiempirical) models. Relating radar backscatter to AGB using empirical models was

achieved with a range of functional forms, including linear [8], [17], [20], [22], logarithmic [23], exponential [18], [23], and higher degree polynomials [3]. In addition, some empirical models were parameterized for backscatter estimation as a function of biomass through sigmoid type functions [12], [24] and subsequently inverted to recover AGB. The semiempirical models [14], [25], [26] were frequently based on the water cloud model [27] and the radiative transfer theory. Finally, some authors have used numerical [28], [29] or nonparametric models [30] to estimate biomass levels.

Past studies have demonstrated the high variability of error in radar predicted biomass with respect to the actual (i.e., field assessed) values. In [5], errors between 39% and 75% were found in boreal forests, depending on the exclusion/inclusion of older stands. In pine forest, stands [8] obtained an average error on the order of 59 t/ha which translates into an error of approximately 80% for forests with an average biomass of 75 t/ha; the inclusion of all stands further increased the error. Sandberg *et al.* [17] estimated biomass in a boreal forest with errors reaching 36%–46% of the mean biomass values. In contrast, relatively low errors (25%) were obtained by Santoro *et al.* [14] in boreal forests, but only when highly homogeneous stands were used. Such studies have reported extensively on the relationship between radar backscatter and forests biomass, but typically for forests with biomass levels well above the L-band saturation point [12], [13], [31] and only occasionally within the sensitivity interval [11], [22]. Consequently, the retrieved biomass intervals were usually much larger than the acknowledged L-band range for biomass sensitivity, making it difficult to assess the retrieval accuracy within those limits. Moreover, limited information is available on the variability of retrieval errors by biomass intervals, which can greatly influence model selection, depending on the specific application and forest biomass distribution frequency.

While many studies have been conducted in boreal, temperate, and tropical environments, fewer studies have focused their attention on low biomass forests in semiarid environments. All studies carried out in semiarid forests used empirical models with no author using more physically based modeling approaches [32]–[35]. Dry conditions are known to enhance wave penetration depth due to decreased vegetation water content, allowing for higher interaction of radar waves with the ground surface and, thus, different scattering mechanisms. In addition, the rate of backscatter increase with biomass is lower in open forests (often the case of semiarid forests) when compared to that in closed canopy forests [36]. Although, semiarid forests frequently present lower biomass levels, which should theoretically yield an increase in the overall estimation accuracy, variations of the surface scattering component (through soil moisture and roughness) could result in similar backscatter levels for a variety of biomass/surface conditions, particularly for copolarized waves [28], [36], which could hinder biomass retrieval.

The aim of this paper was to evaluate the accuracy of different parametric and nonparametric models for biomass retrieval from L-band ALOS PALSAR backscatter data and to demonstrate that by-biomass-interval estimation errors depend little on species composition, forest structure, or field sampling design. The specific objectives were as follows: 1) to assess

the backscatter/biomass relationships for forests characterized by average biomass levels well below the L-band saturation point; 2) to observe the effectiveness of a range of parametric and nonparametric models for biomass retrieval; 3) to study the influence of biomass levels on the retrieval accuracy; and 4) to propose a retrieval strategy that reduces the overall biomass retrieval error (i.e., across the entire biomass range) as well as the error for individual biomass intervals.

II. STUDY AREAS AND DATA SETS

A. Field Data Sets

Field data were available for two study areas corresponding to regional and local forest inventories. At the regional level, the analysis was focused on semiarid pine forests located in the central sector of the Iberian range, Teruel, Spain. The pine species present in the Teruel region were *Pinus sylvestris*, *Pinus halepensis*, *Pinus nigra*, and *Pinus pinaster*. The field work was conducted between December 2004 and April 2005 within the framework of the third Spanish Forest National Inventory (FNI). The sampling grid followed a regular pattern with one sample plot every kilometer within forested areas. All trees with a diameter at breast height (DBH) greater than 7.5 cm were recorded for their DBH and height. The plot radius depended on the maximal DBH at each location: a 5-m radius when the maximum DBH was below 12.5 cm, a 10-m radius when the maximum DBH was between 12.5 and 25.5 cm, a 15-m radius when the maximum DBH was between 25.5 and 42.5 cm, and a 25-m radius when the maximum DBH was above 42.5 cm. The radius of 50% of the 134 plots used in this paper (see Fig. 1) was 15 m, with approximately 25% of the plots having a smaller radius (i.e., 10 m) and 25% of the plots having a larger radius (i.e., 25 m). Only plots located on flat or near flat areas (slope $\leq 5^\circ$) were selected so that results could be easily compared with those from the second study area which is characterized by a nearly flat topography. Moreover, working on flat areas avoided the effect of sloped terrain on biomass retrieval [37] which, according to recent tomographical experiments [38], could enhance the double bounce effect, particularly for copolarized waves [i.e., horizontal transmit/receive (HH)]. The total AGB was calculated for each tree using species-specific allometric equations [39] and aggregated for each plot. The AGB for the selected plots varied between 2.2 and 127.2 t/ha with over 95% of them having an AGB below 100 t/ha. The mean plot biomass was 32.0 t/ha with a standard deviation of ± 26.6 t/ha. The mean tree height was 8.4 m \pm 2.6 m with individual heights varying between 2 and 20 m.

At the local level, the analysis was focused on the Gillenbah forest (1600 ha) located in New South Wales, Australia, where the dominant forest species is white cypress pine (*Calitris glaucophylla*) while gray box (*Eucalyptus microcarpa*) is disseminated throughout the forest and accounts for only 10% of the trees. In September 2011, a biometric survey was conducted using 60 plots (500 m² each) clustered in 12 sites (see Fig. 1). A cluster site consisted of a center plot with four surrounding plots spaced at a distance of 35 m in the cardinal directions. The circumference and height of all trees with DBH greater

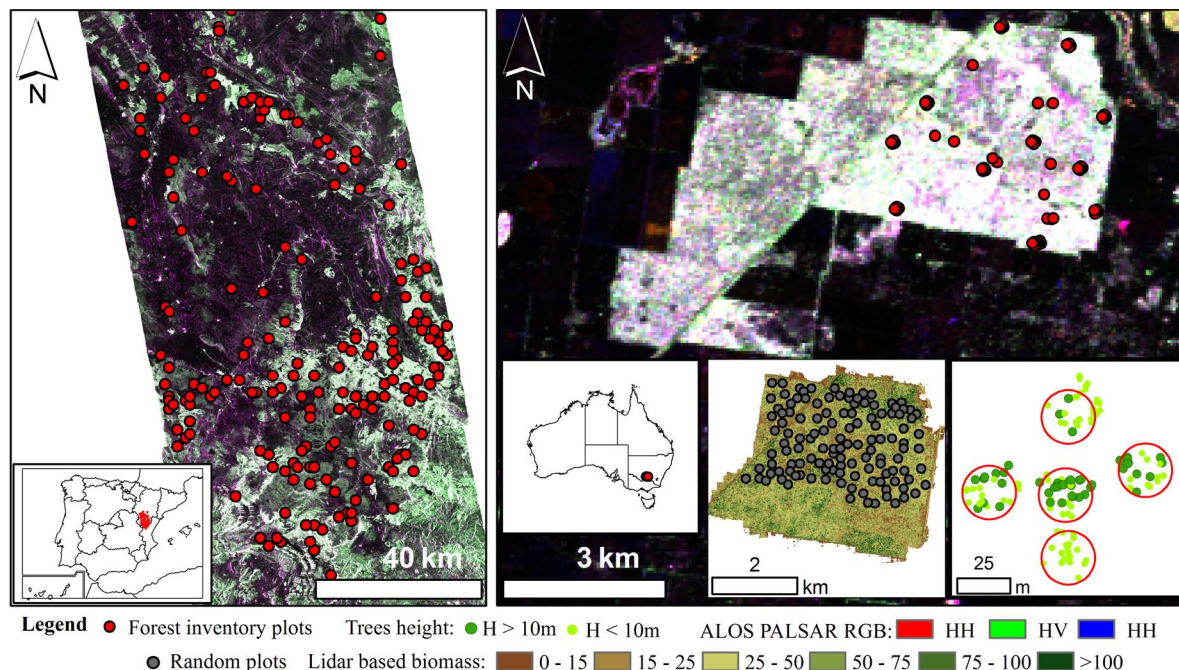


Fig. 1. Location of forest inventory plots for (left) Spanish and (right) Australian study areas, with background of ALOS PALSAR images acquired on (left) July 19, 2008 and (right) May 20, 2010. The insert in the left panel shows the general location of the Spanish study area. The inserts in the right panel show (left) the general location of the Australian study area, (center) the reference biomass levels obtained from lidar data with the random plots used for data extraction, and (right) a typical sampling site with the sampled tree distribution by forest layer. Only plots located on flat or near flat areas are shown for the Spanish study area.

TABLE I

SAR DATA CHARACTERISTICS, PROCESSING PARAMETERS, AND MAIN WEATHER PARAMETERS. FOR THE SPANISH REGION, THE PRECIPITATION RECORDED AT THREE METEOROLOGICAL STATIONS (LOCATED NEAR THE NORTH, THE CENTER, AND THE SOUTH OF THE STUDY AREA, RESPECTIVELY) IS SHOWN, WHEREAS THE MINIMUM AND THE MAXIMUM TEMPERATURE ARE THE AVERAGE FOR THE THREE STATIONS

Parameter	Value	
Study area	Spain	Australia
SAR acquisition date / Scene number	2007.07.17 - KC12666N55N38 2008.06.03 - KC19666N54N38 2008.07.19 - KC20666N57N38	2010.04.04 - ALPSRP223396480 2010.05.20 - ALPSRP230106480 2010.07.05 - ALPSRP236816480 2010.08.20 - ALPSRP243526480
Processing level	L1.5 (slant range intensity)*	L1.1 (complex data)
Acquisition mode	Fine Beam Dual (HH & HV polarizations)	
Multi-look factors	4 range x 16 azimuth	
Pixel spacing	50m	50m
map geometry	UTM30N/ED1950	UTM55S/WGS84
Acc. Pp. (mm)**	[0.0/0.0/0.0], [20.9/20.4/20.4], [0.0/1.1/4.6]	[0.0], [0.0], [4.6], [11.0]
Max/min T (C°)	[33.1/11.4], [19.4/7.7], [34.0/14.3]	[26.8/16.3], [19.3/2.9], [12.7/1.7], [12.7/2.6]

*Format provided for Kyoto & Carbon Initiative / ** Accumulated precipitations recorded for the last 4 days before satellite overpass.

than 5 cm were recorded, whereas smaller trees were counted and their height was estimated plotwise as being the most frequent height (i.e., smaller trees were largely even-aged). Information on grass surface cover and average height from 10 sparsely vegetated plots was also collected. The total AGB was calculated for each tree using species-specific allometric equations [40], [41] and aggregated at plot level.

The forest type over the two study areas was comparable (i.e., largely coniferous species) with average biomass levels well inside the established sensitivity interval for the L-band radar backscatter. However, some differences were noted mostly with respect to the higher biomass levels over the Australian study area and the larger variety of tree species present in the Spanish study area which was not surprising given the latter's much larger extent. Such differences were not viewed as an impediment but rather as an enhancement of this study since

our goal was to assess if similar trends and biomass estimation accuracies are obtained regardless of field sampling design and forest structure. It is also noted that, for the Spanish study area, the minimum DBH recorded was slightly higher (i.e., 7.5 versus 5 cm) and no information on regrowth was available, thereby suggesting a certain underestimation of the actual biomass values.

B. Radar Data Sets

Several dual-polarized (HH and HV) ALOS PALSAR scenes were available for each study area (see Table I). The satellite images, acquired within one to three years of the ground data collection, were multilooked in both range (4) and azimuth (16) to obtain similar ground pixel spacing (50 m). The intensity was transformed to the radar backscatter coefficient (σ°) after

applying the absolute calibration factors [42]. To further reduce speckle noise, the multilooked images were filtered using a 3×3 window [43]. Due to the rough topography, in the Spanish study area, the backscatter intensity was normalized for the varying incidence angle and the effective pixel area [44] using a 20-m spatial resolution digital elevation model (DEM) obtained from the regional government of Aragón. This DEM was assessed as accurate within ± 2.5 m horizontally and ± 5 m vertically. After correction, the gamma nought (γ^0) images only included variations of the scattering properties of the target. Note that, for a flat topography, as was the case for the Australian study site, sigma and gamma nought are equal. Therefore, backscatter normalization was not carried out for the Australian data set. All images were geocoded to the Universal Transverse Mercator (UTM) coordinate system using a lookup table that described the transformation between the radar and the map geometry [45]. The lookup table was generated using the DEM and the orbital information of the radar data. To correct for possible inaccuracies in the input data, a refinement of the lookup table was applied, in the form of offsets between each SAR image and a reference image (e.g., a DEM-based simulated SAR image) transformed to the radar geometry.

Although there was a certain interval between field data collection and satellite image acquisition, no correction was applied to compensate for tree growth. For the Australian study area, the acquisition gap was less than 18 months which meant negligible growth, particularly in such semiarid environments. For the Spanish study area, the acquisition gap was 30 to 42 months. However, according to the third Spanish FNI, the annual average net change in timber volume for pine species in the Teruel region over the past decade was $2.1 \text{ m}^3 \cdot \text{ha}^{-1}$ (i.e., approximately 1 t/ha). Although timber volume is not equivalent to total biomass, such small changes suggest either low annual AGB increments or quasi-equilibrium between tree growth and tree mortality.

C. Data Extraction

For the Spanish data set, the backscatter coefficient was extracted for the pixel containing the center of each ground sampling plot (0.25 ha) which corresponds to the location of the 1-km UTM grid nodes. Such relatively small areas were used to restrain the extraction to the area actually sampled on the ground since no ancillary data were available for the highly fragmented Spanish landscape.

For comparability reasons (i.e., similar speckle noise), the same plot size had to be used to extract the backscatter at the Australian study area. However, the field-assessed plots were much smaller (i.e., 0.05 ha) while forest spatial variability was high. Assigning the field-assessed biomass to a 0.25-ha area centered at each plot would have resulted in a noisier backscatter/biomass relationship. In addition, due to the close proximity of the plots within each cluster site, the 0.25-ha areas would have overlapped. To circumvent such limitations, a reference biomass map was produced using a high point density ($40 \text{ p} \cdot \text{m}^{-1}$) lidar data set from a concurrent with the ground sampling flight. The relationship between field plots (i.e., 60 forests and 10 sparse vegetation) and gridded lidar met-

rics (i.e., pulse density of the 1–12-m height stratum, canopy percent cover in the 6–8-m height stratum, and the volume under the forest canopy surface) was used within multiple linear regressions to model AGB as a function of the lidar metrics. The parameterized model was subsequently applied to obtain a spatially explicit biomass map for the Australian study area. More details on biomass modeling from lidar data are given in [46]. At plot level (i.e., 0.05 ha), the AGB retrieval from lidar point cloud data was accurate within 17.2 t/ha (28% relative). However, when analyzed by cluster site (i.e., 0.25 ha), the retrieval error was significantly lower, i.e., as small as 14% relative to the ground estimates. Biomass values extracted from this biomass reference map were subsequently used for modeling.

A random grid of 131 plots (0.25 ha) was used to extract the radar backscatter and the lidar-based reference biomass over the Australian study area (see Fig. 1). The AGB for the selected random plots varied between 1.5 and 145.6 t/ha with over 95% of them being below 100 t/ha. The mean plot biomass was 50.1 t/ha with a standard deviation of ± 26.5 t/ha. The mean tree height over the Australian study site was $7.2 \text{ m} \pm 2.5 \text{ m}$ with individual heights varying between 2 and 32.5 m.

III. METHODS

A number of modeling approaches can be used to study the relationships between biomass and radar backscatter and to retrieve biomass (i.e., numerical, parametric, and nonparametric modeling). Since numerical modeling requires the detailed description of surface properties (soil roughness and moisture) and vegetation characteristics (leaf/branch orientation, thickness, water content, etc.) to estimate backscatter and such information was not collected during the forest inventory campaigns, the analysis was restricted to parametric and nonparametric models. Although previous studies showed that using multiple polarizations does not significantly improve biomass estimation error [17], [35], it was decided to test not only single-polarized but also multipolarized parametric and nonparametric models to corroborate such results over semiarid low biomass forests.

A. Analysis of the Backscatter–Biomass Relationship

The relationship between radar backscatter was studied as a function of biomass levels using descriptive statistics (i.e., mean and standard deviation of the mean). In addition, the backscatter saturation point with increasing biomass as well as the biomass density below saturation was computed as an average for all available data sets at each study area as proposed in [12]. The backscatter saturation point (linear units) corresponds exactly to the coefficient a of the model (see model 2 in the next section). A 1 dB below the saturation point was considered by Luckman [12] as indicative of the maximum retrievable biomass, taking into account uncertainties in sensor calibration and sample size. In this paper, however, the maximum retrievable biomass was computed for 0.5 dB below saturation since the uncertainty of PALSAR backscatter measurements is smaller and the spatial resolution is higher (i.e., lower speckle noise for the same ground resolution) when compared to JERS data.

B. Biomass Retrieval From Parametric and Nonparametric Models

Six parametric and three nonparametric models were used to retrieve biomass and evaluate the estimation errors. In this paper, the parametric models were further categorized into forward and backward models to distinguish between model parameterization/biomass retrieval strategies. Forward models parameterize the response in backscatter with increasing biomass, hence minimizing the errors of the response variable backscatter. After parameterization, the biomass is estimated using an inverse function. Conversely, in backward models, the AGB is expressed as a function of backscatter without the need of additional functions.

1) *Forward Parametric Models*: The three forward parametric models used [(1)–(3)] were based on the radiative transfer theory and the water cloud model which essentially represents the extinction of microwave radiation as it passes through a layer of vegetation made up of elements containing water [27]. The first model [see (1)] was a semiempirical radiative transfer model of wave propagation through horizontal scattering and attenuating layer [14], [47]

$$\sigma_{\text{for}}^{\circ} = \sigma_{\text{gr}}^{\circ} e^{-\beta \text{AGB}} + \sigma_{\text{veg}}^{\circ} (1 - e^{-\beta \text{AGB}}) \quad (1)$$

where

- $\sigma_{\text{for}}^{\circ}$ total forest backscatter;
- $\sigma_{\text{veg}}^{\circ}$ backscatter from vegetation;
- $\sigma_{\text{gr}}^{\circ}$ backscatter from ground.

Although the parameterization of such models is based on experimental data, the models do take into account (to a certain extent) the physical phenomena (e.g., scattering mechanisms, signal saturation, etc.). This first model, proposed in [14], has the advantage of allowing a straightforward inversion to estimate forest parameters [see (1)]. The total forest backscatter ($\sigma_{\text{for}}^{\circ}$) is modeled as the incoherent sum of direct and vegetation-attenuated ground scattering ($\sigma_{\text{gr}}^{\circ}$) and the direct scattering of the vegetation ($\sigma_{\text{veg}}^{\circ}$). The model takes into account the gaps in the canopy by weighing each term by the area fill factor expressed as a function of the stem-volume-dependent two-way forest transmissivity ($e^{-\beta \text{AGB}}$). The model does not take into account double bounce and higher order reflections, assuming that attenuation through the forest canopy is relevant (which might not be true for low biomass levels) and the forest floor is not perfectly flat. A more thorough description of model assumptions, parameterization, and inversion is given in [14].

In contrast to the original formulation, in this paper, the two-way forest transmissivity was expressed as a function of biomass. Since stem volume can be transformed to biomass by multiplying with species-dependent wood density, for the same moisture content, such a transformation would not affect the two-way forest transmissivity estimates. Furthermore, the total AGB includes the biomass of leaves, branches, and twigs (i.e., the main tree elements interacting with L-band microwaves), therefore providing a better approximation of the total forest transmissivity [i.e., $e^{-\beta \text{AGB}}$ where β is an empirically defined coefficient in (1)]. Although the model was initially developed and tested for copolarized waves, it should be applicable to

cross-polarized waves since the total backscatter is still a mixture of surface and volume scattering but of different magnitudes. The empirically derived forest transmissivity should compensate for differences in scattering mechanisms.

The other two forward models used [see (2) and (3)] were proposed by Luckman [12] and Lucas *et al.* [24], respectively, and are loosely based on the water cloud approach

$$\sigma^{\circ} = a - e^{(-b \text{AGB} + c)} \quad (2)$$

$$\sigma_{(\text{dB})}^{\circ} = a + (\sigma_{\text{gr}(\text{dB})}^{\circ} - a) * e^{-(b \text{AGB})} \quad (3)$$

where

- $\sigma_{\text{gr}(\text{dB})}^{\circ}$ backscatter from ground;
- σ° backscatter coefficient (linear or decibel units);
- a, b, c model coefficients.

The parameter a (i.e., the model asymptote) corresponds to the backscatter saturation point, whereas parameter b describes the gradient of the low biomass density part of the curve. Parameter c and the constant value $\sigma_{\text{gr}(\text{dB})}^{\circ}$ describe the residual backscatter at zero biomass (i.e., the nominal backscatter from bare soil). The models are fitted using calibration data such that the sum of squared deviation from the theoretical curve is minimal. The advantage of such forward models is their robustness when limited samples are available and the potential for allowing residual backscatter at zero biomass density (i.e., allowing for soil surface scattering at low biomass levels) [12]. Model (3) assumes a fixed value for the ground backscatter ($\sigma_{\text{gr}}^{\circ}$) which, in this paper, was estimated as the average of all samples with biomass levels below 10 t/ha. Such sigmoid functions were often used to study the biomass–backscatter relationships, determine the dynamic range of the data, and calculate the level of signal saturation [11], [12], [15], [24].

After model parameterization, biomass was retrieved by analytically inverting models (1)–(3) as in

$$\text{AGB} = -\frac{1}{\beta} \ln \left(\frac{\sigma_{\text{veg}}^{\circ} - \sigma_{\text{for}}^{\circ}}{\sigma_{\text{veg}}^{\circ} - \sigma_{\text{gr}}^{\circ}} \right) \quad \text{inversion function for (1)}$$

$$\text{AGB} = \frac{[-\ln(a - \sigma^{\circ}) - c]}{b} \quad \text{inversion function for (2)}$$

$$\text{AGB} = -\ln \frac{\sigma_{(\text{dB})}^{\circ} - a}{\sigma_{\text{gr}(\text{dB})}^{\circ} - a} \times \frac{1}{b} \quad \text{inversion function for (3)}$$

When inverting, rules need to be defined for validation plots having backscatter values that fall outside of the modeled interval. The direct assignment of the minimum and maximum biomass values measured in the area of interest was proposed in [14] when the backscatter intensity values fall below or above the modeled intervals, respectively. In this paper, however, such values were simply discarded from inversion since our objective was not to produce a spatially explicit biomass map but rather to analyze the errors of different retrieval models. Retaining such values would have defeated the purpose of the study since the estimation error would have been a function of the number and distribution of such outliers for each particular parameterization. The models were applied to all data sets and polarizations.

2) *Backward Parametric Models*: Three backward parametric models [see (4)–(6)] were also used to retrieve biomass levels, and their accuracy was estimated for each available study area and SAR image at both HH and horizontal transmit and vertical receive (HV) polarizations. A dual-polarization model form was also used [see (6b)] to assess the potential advantages of jointly using copolarized and cross-polarized information. Backward models have the advantage that regression coefficient estimation is straightforward and the statistical properties of the estimates are well understood

$$\text{AGB}^\lambda = a + b\sigma_{\text{dB}}^\circ \quad (4)$$

$$\text{AGB} = ae^{b\sigma^\circ} \quad (5)$$

$$\log(\text{AGB}) = a + b\sigma_{\text{dB}}^\circ + c\sigma_{\text{dB}}^{\circ 2} \quad (6)$$

$$\log(\text{AGB}) = a + b\sigma_{\text{xx}}^\circ + c\sigma_{\text{xx}}^{\circ 2} + d\sigma_{\text{xy}}^\circ(\text{dB}) + e\sigma_{\text{xy}}^{\circ 2}(\text{dB}) \quad (6b)$$

where

σ° backscatter coefficient (linear or decibel units);
 σ_{xy}° backscatter coefficient (decibel units) for xy transmit/receive combination;

a, b, c, d, e model coefficients;

$\lambda = 0.5$.

The linear model relating the squared root (or similar power) transformation of the biomass and the backscatter coefficient [see (4)] was proposed in [17]. The model form and the independent variables included were obtained after an iterative optimization process (see [17] for more details on model parameterization). For this paper, the parameter λ proposed in [17] is used for single-polarized data. The next model [see (5)] is an exponential type function. Such functions are frequently used to model biomass change with increasing backscatter [18], [23]. The model in (6) was proposed by Saatchi *et al.* [48] and is based on backscattering information from fully polarized systems that provide independent measurements of forest structure and biomass. The quadratic form of the model reproduces the loss of radar backscatter sensitivity in higher biomass forests. The model has been adapted to work with single- and dual-polarized data sets by stripping out terms related to polarizations not acquired by the ALOS PALSAR sensor [see (6) and (6b)]. These modified models represent roughly one or two scattering mechanisms, depending on the polarization/s used (i.e., stem-surface/crown volume and crown volume scattering for HH and HV polarizations, respectively).

The backward models were parameterized using least squares optimization, and biomass retrieval was carried out over the entire validation data set. It is noted that such models do not limit biomass retrieval based on defined backscatter thresholds, which results in a biomass value being computed for each sample regardless of its backscatter.

3) *Nonparametric Models*: Three nonparametric models (i.e., ensemble regression (ER), random forest (RF) regression, and support vector machine (SVM) regression) were used to estimate the biomass retrieval accuracy. Ensemble learning techniques use multiple models to improve the predictive power with respect to any of the constituent models by aggregating their predictions. Multiple models are generated based on the training data set and subsequently pruned and integrated. The least square boost ensemble was used to incrementally build

the ensemble by training new model instances using weak learners. The returned model structure was adjusted through 100 learning cycles and used in predicting responses to data. RF regression [49] uses similar ensemble learning methods by constructing a large number of decision trees from the training data which are subsequently used to derive overall predictions as the average response from all individually trained trees. Compared with ER and RF regression, data sets used for SVM regression [50] need to be rescaled and modified to achieve accurate predictions. The produced model is also sensitive to the SVM regression parameters. In this paper, SVM regression was based on a radial basis kernel function (i.e., able to handle nonlinear relationships), and the related parameters were optimized by grid search. The values were scaled to the 0–1 interval prior to model construction. The nonparametric models were trained using single- or dual-polarization data as predictor variables and the observed AGB as the corresponding response. All models were parameterized using the entire biomass range and applied to the validation data sets to compute the biomass retrieval accuracy metrics.

C. Combined Parametric Models

To increase biomass estimation accuracy within the biomass intervals of interest (0–100 t/ha) while retaining the overall accuracy, a combination of backward and forward parametric models was proposed. In the first instance, both forward (e.g., model 1) and backward (e.g., model 6) models are parameterized, and the biomass is estimated independently. The biomass values obtained from the backward model are retained only within the physically realistic retrieval interval as parameterized by the forward model (e.g., $\sigma_{\text{veg}}^\circ$ and σ_{gr}°). A backscatter threshold corresponding to a user-defined biomass level (e.g., 5, 10, and 30 t/ha) is calculated based on the parameterized forward model. This backscatter threshold is subsequently used to retain the final biomass values: 1) For backscatter values above the threshold, the biomass estimates from the backward model are retained, and 2) for backscatter values below the threshold, the biomass estimates from the forward model are retained. By changing the backscatter threshold, the relative importance of the backward and the forward model, respectively, for the final biomass estimation is controlled.

D. Error Analysis

Cross-validation techniques are often used to compare the performance of different predictive models. Repeat random subsampling with cross-validation was used to assess biomass retrieval accuracy. To reduce the variability due to random sampling effects, 25 rounds were performed by splitting the data sets into training (60%) and validation (40%) samples. During each round, the models were parameterized based on the training samples and subsequently used to estimate the biomass of the validation samples. Biomass retrieval accuracy was described using four error metrics: the root-mean-squared error (RMSE), the relative RMSE, the average error (bias), and the correlation coefficient (r) between the measured and the retrieved AGB. In addition, a relative estimation error (RE%)

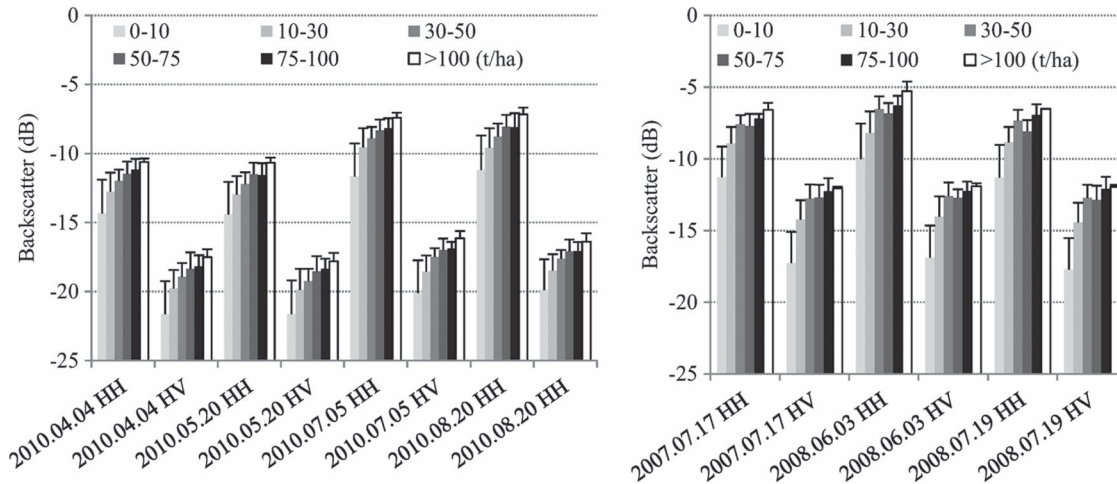


Fig. 2. Average L-band radar backscatter by biomass intervals for (left panel) Australian and (right panel) Spanish study areas. The vertical bars represent the standard deviation of the mean.

was calculated for each validation sample [see (7)] and averaged by biomass intervals

$$RE_{\%} = 100 * |AGB_{\text{observed}} - AGB_{\text{predicted}}| / AGB_{\text{observed}} \quad (7)$$

Although the relative error metric suffers from instability when approaching zero biomass values (i.e., as the denominator approaches zero the relative error approaches infinity), we consider its use valuable, particularly when assessing the biomass error by retrieval intervals where other metrics (i.e., absolute error) are less meaningful. For example, an absolute estimation error of 5 t/ha could be considered as acceptable for higher biomass intervals (e.g., 50–100 t/ha) but would represent a significant deviation from the true value at lower biomass intervals (e.g., 0–10 t/ha).

The error metrics for biomass estimation were computed for each SAR acquisition date and polarization from predicted values and their corresponding observed values accumulated over the 25 iterations. Such averages provided a measure of model sensitivity to random sampling effects (i.e., the input training data set). The standard deviation of the errors provided a measure of random sampling effects on the retrieval accuracy. In addition, the error metrics were averaged by study area (i.e., using all SAR acquisition dates) for the same polarization to provide a synopsis of the expected retrieval accuracy for each model. The standard deviation of the multitemporal averages provided a measure of the temporal stability of the error metrics (i.e., a measure of changing environmental condition effects).

IV. RESULTS

In semiarid environments, a large part of the scattering comes from the forest floor (due to the open canopy structure and relatively low biomass levels), and the environmental conditions could strongly influence the scattering mechanisms. In this paper, images acquired during dry and wet periods were used to study the potential influence of such effects on the retrieval accuracy. The smaller extent (16 km²) of the Australian study site and the almost flat topography guaranteed little spatial variations in the environmental conditions for each acquisition date. For the Spanish study site, however, such spatial

variation could be present due to the considerably larger area (10 000 km²).

A. Analysis of the Backscatter–Biomass Relationship

The relationship between radar backscatter and biomass density was assessed using six biomass intervals. The first interval (i.e., 0–10 t/ha) corresponds to sparsely vegetated areas where the ground contribution is large. The second and third intervals (i.e., 10–30 and 30–50 t/ha) correspond to an increasing proportion of the volume scattering and a reduction of the ground component due to signal attenuation, whereas for the remaining intervals (i.e., 50–75, 75–100, and > 100 t/ha), the volume scattering component dominates and signal saturation appears. The AGB levels for the sites used in this paper ranged between 1.5 and 145.6 t/ha, with most of the plots being below the maximum saturation limit of L-band estimated at 100 t/ha [3]. Fig. 2 reports the mean value and standard deviation of the backscatter for each biomass interval (in decibels) calculated for each data set and polarization in both study areas. The spread of the measurements around the mean indicates backscatter heterogeneity due to surface characteristics (i.e., soil moisture and surface roughness), forest structure, vegetation water content, and the sensitivity of the backscatter to AGB. The total dynamic range was between 4 and 6 dB for HH and HV polarizations, respectively. However, the dynamic range between adjacent biomass intervals was significantly lower. The highest value, 2–3 dB, was recorded between the two lowest biomass intervals (0–10 and 10–30 t/ha). With increasing biomass, the mean backscatter difference between subsequent classes decreases with the highest biomass classes being separated by less than 1 dB. The highest standard deviation (2.5 dB) was recorded for the lowest biomass interval for both polarizations which could be explained by a significant influence of the underlying surface properties. With increasing AGB, the backscatter variability decreased to less than 0.5 dB for the highest biomass interval.

After rainfall events, backscatter increases by up to 3 dB for the HH polarization and 1 dB for the HV polarization for the Australian study area (see left panel of Fig. 2 for July 05,

TABLE II
SATURATION POINT AND BIOMASS DENSITY BELOW SATURATION POINT
FOR AUSTRALIAN AND SPANISH STUDY AREAS. THE VALUES WERE
COMPUTED AS IN [12] AND REPRESENT AVERAGES FOR
ALL SAR ACQUISITION DATES

Area	SAR metric	Saturation point (dB)	Biomass density 0.5 dB below saturation (t/ha)
Australia	HH	-8.9	56.1 ± 1.6
	HV	-17.1	58.6 ± 1.4
Spain	HH	-6.9	35.6 ± 1.1
	HV	-12.2	43.1 ± 1.0

2010 with Acc.Pp. = 4.6 mm and August 20, 2010 with Acc.Pp. of = 4.6 mm). For the Spanish study area, backscatter levels after rainfall events increased by only 1 dB (see right panel of Fig. 2 for June 03, 2008 with Acc.Pp. = 20.6 mm). The smaller increase was likely caused by the spatial patterns of rainfall due to the much larger area analyzed. Notably, rainfall events did not affect backscatter dynamic range and by-biomass-interval variability which was reflected in similar biomass retrieval accuracies regardless of the environmental conditions as demonstrated in the next sections. The estimated saturation point and biomass density below saturation computed as in [12] are presented in Table II. Different saturation points were observed for the two study areas with higher values being recorded for the Spanish data set. Such differences were explained by the generally higher backscatter levels at both polarizations observed for the Spanish data sets over forest or other land cover types. The biomass density below saturation was higher for the Australian study area by an average of 18 t/ha.

B. Error Analysis for the Entire Biomass Range

Daily RMSE for all SAR data sets is presented in Fig. 3 for single-polarized models. For each day, the RMSE was averaged over the 25 independent iterations. The standard deviation was calculated to provide a measure of result variability on the samples selected for model parameterization. The RMSE varied around 24 ± 1.9 t/ha and 21 ± 2.2 t/ha for the Australian and Spanish study areas, respectively, at both polarizations. When analyzed by model, the day-to-day change in RMSE was usually below 2 t/ha, suggesting fairly stable retrieval accuracy regardless of the environmental conditions for both study areas. Small daily changes of the standard deviation (< 2 t/ha) also suggested that environmental conditions had little effect on biomass retrieval metrics. It is noted that similar results were obtained for the dual-polarization models (data not shown).

The low sensitivity of the RMSE to environmental effects suggested that overall error metrics could be computed for each area, taking into account all SAR acquisition dates. Therefore, average values for RMSE, relative RMSE, r , and estimation bias were computed for each study area to provide a synopsis of the expected retrieval accuracy for each model (see Fig. 4). No consistent trend was observed among different models for the RMSE and relative RMSE metrics. One model (model 3) appeared to consistently outperform all remaining models, although by small margins (3–4 t/ha and 7%–10% lower for

RMSE and relative RMSE, respectively), in both study areas and for both polarizations. In general, the average relative RMSEs were between 40% and 80%, which is comparable to previously reported results [8], [16]. More interesting trends were observed when analyzing the correlation between the observed and the predicted biomass (r). Forward models consistently provided the lowest r values in both study areas and for both polarizations. Average r values over both study areas and polarizations were 0.48 for the forward models, 0.61 for the backward models, and 0.58 for the nonparametric models. Similar trends were observed for the estimation bias with the forward models having the highest bias. One model in particular, model 3, underestimated the biomass by an average of 10 t/ha. The smallest bias (< 1.5 t/ha) was observed for the two nonparametric models based on ensemble regression (i.e., ER and RF). Using two polarizations consistently improved all error metrics, although only by small margins. These results support previous findings [17], [35] which found no significant improvement in biomass estimation when using two polarized models. However, two polarized nonparametric models (i.e., ER and RF) provided almost unbiased biomass estimates.

C. Error Analysis by Biomass Intervals

The relative estimation error (RE%) was further studied by biomass intervals (see Fig. 5). The highest estimation error was consistently associated with the lowest biomass interval (0–10 t/ha), despite its higher dynamic range. With increasing biomass, the errors decreased significantly for biomass intervals around the saturation point after which the estimation error starts increasing. Similar results were obtained when simultaneously using two polarizations (see Fig. 6). The higher relative estimation error observed for the lowest biomass interval could be the result of two factors: the high signal variability due to the influence of local surface conditions (i.e., roughness and moisture) and the instability of the RE% metric as explained in the previous section. Modeling studies showed that, in low biomass areas, direct scattering from the ground dominates the signal [51] with the volume scattering having a much lesser role. The higher backscatter standard deviation for the lowest biomass interval (i.e., 0–10 t/ha) observed for our study areas (see Fig. 2) supports previous findings, suggesting that biomass estimation errors in this interval depend mostly on the local surface conditions. Note that forward models provided lower estimation errors for the lowest biomass interval, partially due to the model inversion constraints which limit retrieval below a certain backscatter threshold (e.g., $\sigma_{gr}^{\circ}(\text{dB})$ and σ_{gr}°). When using backward and nonparametric models, however, no constraints are imposed with biomass retrieval being carried out for all validation plots.

D. Error Analysis for Combined Model Retrieval

Fig. 7 presents the results of a combined retrieval method using initial estimates from forward (model 1) and backward (model 6) models. Similar results, not shown, were obtained when using other combinations of forward and backward models. A backscatter threshold corresponding to 10 t/ha was used

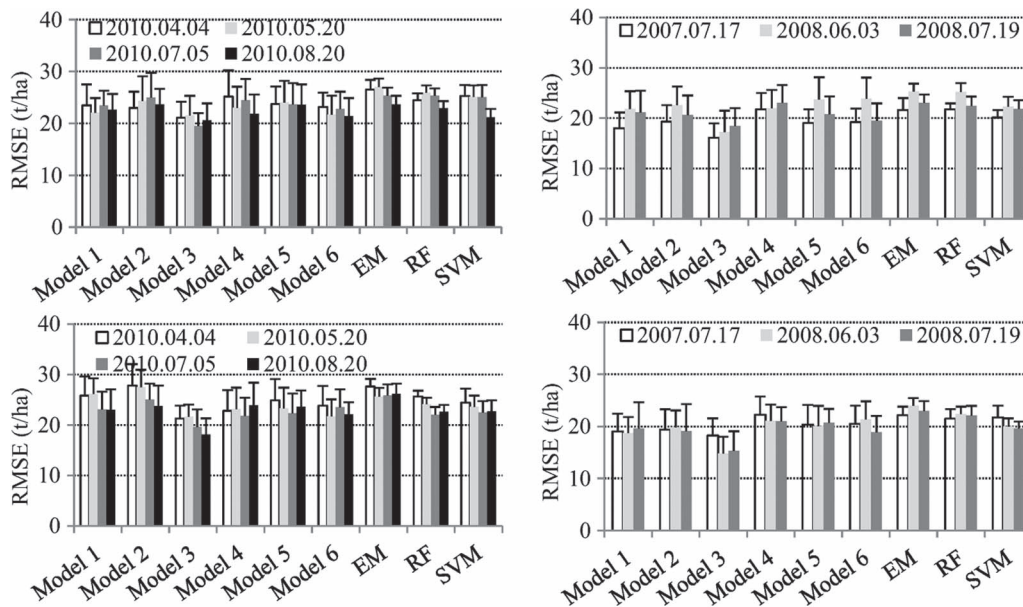


Fig. 3. Biomass estimation error (RMSE) for each SAR data set for (left panels) Australian and (right panels) Spanish study areas. Upper panels show HH polarization while bottom panels show HV polarization.

to separate the backscatter values and retain the corresponding biomass estimates: For backscatter below the threshold, the biomass estimated from the forward model was retained, while for backscatter above the threshold, the biomass estimated by the backward model was retained. The improvement in retrieval accuracy was evident when compared to initial models, particularly when looking at specific intervals. Using the combined approach, the higher accuracy of the model proposed in [14] was largely retained for the lowest biomass levels (0–30 t/ha) while increasing the estimation accuracy for the higher biomass levels (30–100 t/ha) by around 10%–20% with respect to the forward models. In addition, the overall error in the 10–100 t/ha interval was typically improved with respect to the forward model by 5%–15%, depending on the study area and polarization. One should notice, however, that such improvements come at the cost of discarding some of the backscatter values before retrieval. Therefore, such retrieval strategies would imply labeling pixels outside the modeled interval (as estimated by forward models) as nonretrievable, which would result in patchy biomass maps. For our study areas, the number of values discarded varied up to 25% of the total number of samples.

V. DISCUSSIONS

Study areas with different species composition were selected to assess if similar trends and estimation errors are obtained for a variety of situations and independently of the ground sampling strategy. Analyzing a relatively small forest (16 km²) with limited species variability (i.e., Australian site) allowed the exclusion of potential errors due to spatial variability in environmental conditions. The Spanish study area was instead characterized by species heterogeneity and spatial variability since a regional sized data set was used (10 000 km²).

The backscatter dynamic range for both study areas was lower when compared to values reported in [11] while it was

close to the values reported in [17]. Note that backscatter dynamic range is significantly influenced by the selection of the low biomass sample plots. Frequently, such plots are located in nonforested areas such as bare agricultural fields which could present significantly lower backscatter due to reduced surface roughness which favors specular scattering. For both study areas, more than two-thirds of the dynamic range corresponded to the lowest biomass interval (0–30 t/ha), while for the remaining interval (30–100 t/ha), the dynamic range was around 1–2 dB, depending on polarization, which could explain, to a certain extent, the difficulties encountered by many studies when retrieving biomass using L-band backscatter. The backscatter range at which signal saturation occurs was within previously reported intervals [11], [12], although such values are likely to fluctuate with sensor calibration and local conditions. The biomass density below saturation point was higher for the Australian study area (57 t/ha) when compared to the Spanish study area (39 t/ha). Nevertheless, both values were within previously observed ranges [11], [12], [24].

Reported biomass retrieval accuracy metrics are frequently limited to RMSE with fewer authors providing information on the relative RMSE, the estimation bias, or the correlation between predicted and observed values. Although RMSE is an important metric, by itself, it is not sufficient for a comprehensive error characterization. Relative RMSE provides additional information of estimation precision since the performances of models applied over variable biomass ranges could be more easily compared. Additional metrics such as the estimation bias and the correlation between predicted and observed values (r) could be useful for selecting the most appropriate model since different models could present similar RMSE or relative RMSE values (see Section IV). In this paper, the observed RMSE was around 20 t/ha regardless of the study area with the relative RMSE varying around 40%–50% for the Australian study area and 60%–80% for the Spanish study area. The difference in relative RMSE values between the two study areas was attributed

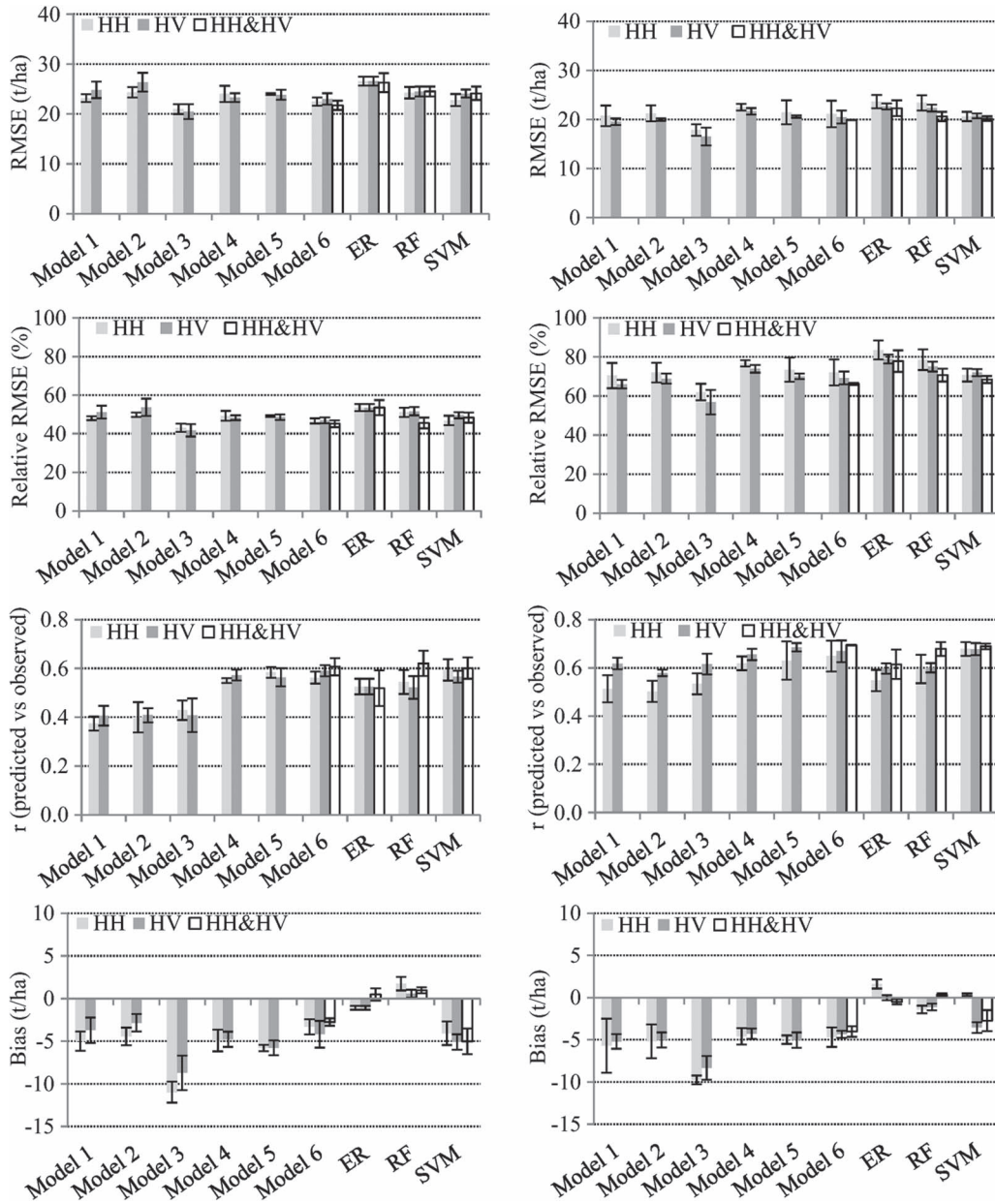


Fig. 4. Model-dependent estimation error metrics (RMSE, relative RMSE, r , and bias). The metrics are given for each model and polarization for the (left) Australian and (right) Spanish study areas. The values represent averages of all SAR acquisition dates. The vertical bars represent the standard deviation among individual days. Two equations were used to produce the result labeled Model 6: Single-polarized models were based on (6) while dual-polarized models were based on (6b), which adds two terms corresponding to the second polarization.

to the larger sample variability at the Spanish study site due to the increased number of species and the much larger area covered by the forest inventory (i.e., spatial variability of the environmental conditions). The correlation between observed and predicted values (r) was between 0.4 and 0.7, depending mostly on polarization and retrieval model. The estimation bias was generally below 5 t/ha except for model 3 which underestimated the biomass level by an average of 10 t/ha.

This paper also showed that forest biomass retrieval accuracy from radar backscatter observations is highly variable within the L-band sensitivity range. In particular, considerably larger errors were observed for all models at both ends of the sensitivity interval, i.e., when approaching 0 and 100 t/ha. Despite the high backscatter dynamic range, forest biomass retrieval was

most likely hindered by surface properties for the low biomass levels (i.e., < 30 t/ha). If surface properties are not taken into account, incorrect estimation is expected in low biomass areas, particularly for long wavelengths. For midrange biomass intervals (30–75 t/ha), better retrieval accuracy (20%–35%) was achieved by using backward parametric models with nonparametric and forward models providing slightly higher estimation errors (i.e., 30%–40% and 40%–50%, respectively). At higher biomass levels (i.e., > 100 t/ha), signal saturation could be overcome by using longer wavelengths. The use of P-band data could increase the saturation point to about 200 t/ha [3], [5] and thus increase the retrievable biomass interval. However, the higher penetration at P-band would also increase the surface scattering contribution to the total backscatter at midrange

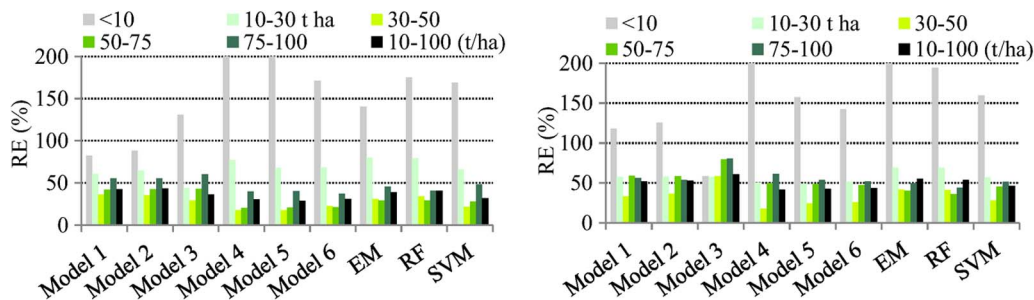


Fig. 5. Relative biomass estimation error (RE%) by biomass intervals for single-polarized (HH polarization) models for the (left panel) Australian and (right panel) Spanish study areas. The values represent averages of all SAR acquisition dates.

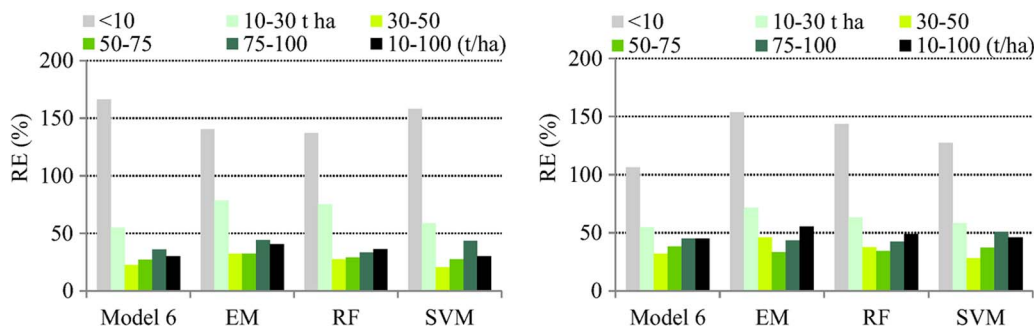


Fig. 6. Relative biomass estimation error (RE%) by biomass intervals for dual-polarized models. (Left panel) Australian study area and (right panel) Spanish study area. The values represent averages of all SAR acquisition dates. The results labeled Model 6 were based on (6b).

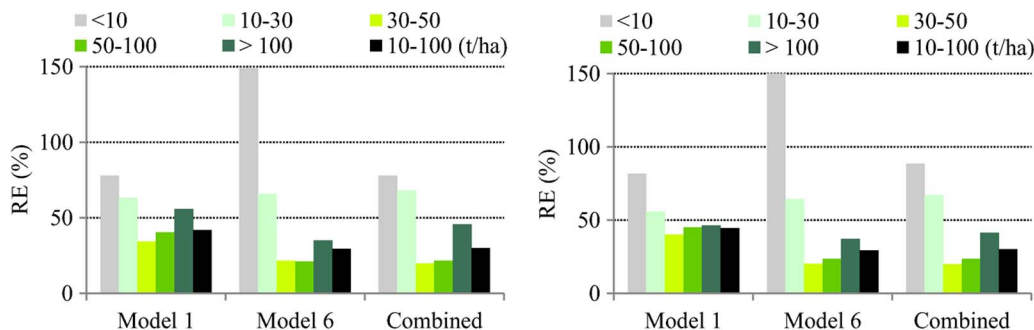


Fig. 7. Relative biomass estimation error (RE%) using a combined model for the Australian study area. Left panel represents HH polarization, and right panel represents HV polarization. The values represent averages of all SAR acquisition dates.

biomass densities. Without information on surface characteristics from SAR or ancillary sensors, forest biomass retrieval in degraded or regenerating forests could bear significant errors.

Using forward semiempirical models (e.g., model 1), the main scattering components can be estimated as well as the signal attenuation through the forest canopy which allows the examination of the relative importance of ground and volume scattering components. A further advantage of such methods resides in the opportunity to limit the biomass retrieval to a physically valid backscatter interval which decreases the estimation error at low biomass levels. The main drawback of the semiempirical and empirical forward models is the need for inverse relationships to retrieve biomass values. This has a significant influence on the retrieval errors since the model parameterization is based on least squares regression which minimizes the sum of squared distances from each observation to the fitted line. Forward models parameterize the response in backscatter with increasing biomass, hence minimizing the errors of the response variable backscatter. For the backward

models, however, this distance corresponds to the response variable AGB, which explains the generally higher estimation accuracies (with the exception of the lowest biomass intervals). However, none of the studied models consistently outperformed the remaining ones when considering overall values for each error metric. Nonetheless, some general conclusions could be drawn since backward and nonparametric models consistently outperformed forward models when analyzing the correlation between predicted and observed values, while two of the nonparametric models (i.e., ER and RF) presented almost no estimation bias. When analyzing retrieval errors by biomass intervals, it was evident that forward models were more accurate at low biomass levels while backward models showed considerably better results for intermediate biomass levels. The combined retrieval strategy proposed in this paper has taken advantage of the different model strengths to decrease the overall and by-biomass-interval RMSEs by up to 5%–15% and 10%–20%, respectively. Such a retrieval strategy can be used to gear the retrieval toward obtaining the most accurate

biomass estimate at either ends of the sensitivity spectrum, depending on the specific application. For example, given a pre-existing classification, one could gear the algorithm for higher accuracies at low biomass intervals in regrowth areas while maintaining high retrieval accuracies for the higher biomass levels in mature forests.

Parametric and nonparametric models implicitly incorporate the dielectric properties of the vegetation and the underlying surface [52]. Since these properties are known to vary in space and time, relationships derived for a specific data set are not easily transferable—one of the major drawbacks of such retrieval methods. Even for similar environmental conditions (i.e., dry), significantly different model parameters were found between study areas, acquisition dates, and polarizations, which suggests that estimation errors would increase when applying models parameterized for different satellite data sets or regions. Numerical models [28], [29] have the potential to improve model transferability between areas by taking into account additional parameters such as surface properties and vegetation structural parameters (e.g., water content, leaf/branch orientation, etc.). Unfortunately, such detailed information is not readily available from existing field campaigns or forest inventories and so has to be retrieved from independent sources. In addition, interactions between microwaves and media depend not only on the easier-to-generalize vegetation structural properties (e.g., length and orientation of branches, leaf shape and size, etc.) but also on the vegetation water content which changes along the canopy, thereby partly explaining the relatively low prediction accuracy (RMSE of 1.5 to 8 dB for HH and HV polarizations, respectively) obtained from such approaches. With a dynamic range for dense vegetation (i.e., > 30 t/ha) of only 2–3 dB, the numerical models lack the accuracy needed for forest biomass retrieval, making parametric and nonparametric models still relevant for the remote sensing community.

When compared to previous studies, the results were often divergent. For example, in [14], the first model (model 1) was used to retrieve biomass from L-band HH data over coniferous dominated boreal forests with estimation accuracy metrics ranging between 36–102 t/ha (RMSE), 25%–51% (relative RMSE), and 0.56–0.87 (r). While the RMSE observed in this paper was considerably lower, most likely due to the lower biomass levels, the relative RMSE and r metrics were slightly worse. The reduced accuracy could be related to the smaller sample size (i.e., 0.25 ha) used in this paper when comparing to the significantly larger sample plots (i.e., 0.5 to 20 ha or larger) used in [14]. Smaller sampling plots are related to an increased forest variability which, in turn, negatively affects biomass retrieval accuracy since similar backscatter values could stem largely from different forest structures. In [17], a linear model (model 4) was used to retrieve biomass over hemiboreal coniferous forests, while in [18], an exponential model (model 5) was used over tropical forests. The RMSE and relative RMSE observed were around 70–80 t/ha and 40%–45% (HH and HV polarizations) for the hemiboreal forests. For the tropical forests, the RMSE ranged from 100 to 150 t/ha with a negative bias around 50 t/ha. Again, the much higher RMSE observed in these studies was most likely related to mean biomass values in excess of 150 t/ha. It is noted that it is difficult to pinpoint

the origin of result incongruence even when applying the same model since previous studies were carried out over forests greatly exceeding the widely acknowledged L-band biomass sensitivity interval (i.e., < 100 t/ha), using plots of varying size and with reference data of variable accuracies (i.e., up to 95-t/ha estimation error for reference biomass values [18]). In addition, for the forward models, rules have to be decided for backscatter values outside of the retrievable interval which further distort the error metrics and, thus, any comparison.

In earlier studies, radar backscatter was shown to provide better relationships with biomass levels at coarser spatial resolution and/or within a multitemporal approach [53], [54]. Such studies demonstrated that SAR-based biomass retrieval could achieve the precision required for global, continental, or regional scale (i.e., boreal or tropical region) applications. The relatively high accuracy obtained in such studies was related to the low spatial resolutions at which such regional maps are produced (1–10-km pixel spacing), which dramatically improves the accuracy of both the backscatter coefficient estimates (i.e., high number of looks) and field biomass sampling (i.e., decreased forest variability). The approach described in [54] could be applied to the wealth of SCANSAR data available from ALOS PALSAR, but such an approach would produce appropriate results only when estimates at coarse spatial resolution are required. However, for forest management purposes, high spatial resolution (i.e., 100-m pixel spacing or better) products are necessary since forest stands can be as small as 1 ha in highly fragmented areas. The results here have shown that relatively high estimation accuracy (down to 20%) can be achieved at plot level at least for some biomass intervals. At stand level, improvements of the estimation errors are expected since such analysis would benefit from the smaller errors associated to lower forest spatial variability, decreased speckle, and more accurate field estimates since larger areas proved to be less prone to errors due to the expansion of field-measured forest parameters.

VI. CONCLUSION

This paper has analyzed the SAR backscatter response from two forested areas located in semiarid environments and studied overall and by-biomass-interval retrieval errors using a range of parametric and nonparametric models. The sensitivity of L-band radar backscatter to variations in AGB over areas of similar environmental conditions but with different forest species composition and field sampling strategies was explored, demonstrating that our findings were not of random nature but genuine trends independent of the local conditions. For both study areas, the backscatter coefficient increased asymptotically with biomass from the minimum values associated with sparsely vegetated areas. Although overall dynamic ranges varied within expected values, different trends were observed when analyzing by biomass intervals, with most of the dynamic range corresponding to low biomass intervals. For the remaining biomass intervals up to the L-band saturation point, the backscatter dynamic range was considerably smaller.

This paper also showed that the retrieval accuracy of forest biomass from L-band radar backscatter observations is highly

variable when different biomass intervals are considered. In particular, larger errors were observed at both ends of the L-band biomass sensitivity interval. At very low biomass levels, information on surface properties is needed to increase the estimation accuracy, whereas at higher biomass levels, signal saturation dominates and the estimation accuracy starts to degrade.

Overall, biomass retrieval errors were largely similar for the entire range of parametric and nonparametric models studied. However, forward models consistently provided the lowest correlation between the observed and the predicted biomass while nonparametric models generally provided unbiased estimation. When analyzing by biomass intervals, forward models consistently outperformed backward and nonparametric models at low biomass levels (i.e., < 30 t/ha), while at intermediate biomass levels (30–75 t/ha), backward models were the most accurate (relative RMSE of 20%–35%), closely followed by nonparametric models. To increase biomass retrieval accuracy, a strategy based on combining different model types was proposed. Such a retrieval strategy had the potential to reduce both overall and by-biomass-interval errors by up to 15%–20%.

ACKNOWLEDGMENT

The authors would like to thank Dr. M. Santoro and Dr. J. Hacker for facilitating this work.

REFERENCES

- [1] H. K. Gibbs, S. Brown, J. O. Niles, and J. A. Foley, "Monitoring and estimating tropical forest carbon stocks: Making REDD a reality," *Environ. Res. Lett.*, vol. 2, no. 4, pp. 045023-1–045023-13, Oct.–Dec. 2007.
- [2] J. Riom and T. Le Toan, "Relations entre des types de forêts de pins maritimes et la rétrodiffusion radar en bande L," in *Proc. Spectr. Sign. Obj. Remote Sens. Symp.*, Avignon, France, 1981, pp. 455–465.
- [3] M. C. Dobson, T. Ulaby, T. Le Toan, A. Beaudoin, and E. S. Kasischke, "Dependence of radar backscatter on coniferous forest biomass," *IEEE Trans. Geosci. Remote Sens.*, vol. 30, no. 2, pp. 412–415, Mar. 1992.
- [4] E. S. Kasischke, N. L. Christensen, and B. J. Stocks, "Fire, global warming, the carbon balance of boreal forests," *Ecol. Appl.*, vol. 5, no. 2, pp. 437–451, May 1995.
- [5] E. J. Rignot, J. Way, C. Williams, and L. Viereck, "Radar estimates of aboveground biomass in boreal forests of interior Alaska," *IEEE Trans. Geosci. Remote Sens.*, vol. 32, no. 5, pp. 1117–1124, Sep. 1994.
- [6] T. Le Toan, A. Beaudoin, and D. Guyon, "Relating forest biomass to SAR data," *IEEE Trans. Geosci. Remote Sens.*, vol. 30, no. 2, pp. 403–411, Mar. 1992.
- [7] P. A. Harrell, L. L. Bourgeau-Chavez, E. S. Kasischke, N. H. F. French, and N. L. Christensen, "Sensitivity of ERS-1 and JERS-1 radar data to biomass and stand structure in Alaskan boreal forest," *Remote Sens. Environ.*, vol. 54, no. 3, pp. 247–260, Dec. 1995.
- [8] P. A. Harrell, E. S. Kasischke, L. L. Bourgeau-Chavez, E. M. Haney, and N. L. Christensen, "Evaluation of approaches aboveground biomass in using SIR-C data to estimating southern pine forests," *Remote Sens. Environ.*, vol. 59, no. 2, pp. 223–233, Feb. 1997.
- [9] M. L. Imhoff, "Radar backscatter and biomass saturation: Ramifications for global biomass inventory," *IEEE Trans. Geosci. Remote Sens.*, vol. 33, no. 2, pp. 511–518, Mar. 1995.
- [10] E. S. Kasischke, N. L. Christensen, and L. L. Bourgeau-Chavez, "Correlating radar backscatter with components of biomass in Loblolly pine forests," *IEEE Trans. Geosci. Remote Sens.*, vol. 33, no. 3, pp. 643–659, May 1995.
- [11] R. Lucas, J. Armston, R. Fairfax, R. Fensham, A. Accad, J. Carreiras, J. Kelley, P. Bunting, D. Clewley, S. Bray, D. Metcalfe, J. Dwyer, M. Bowen, T. Eyre, M. Laidlaw, and M. Shimada, "An evaluation of the ALOS PALSAR L-band backscatter—Above ground biomass relationship Queensland, Australia: Impacts of surface moisture condition and vegetation structure," *IEEE J. Sel. Topics Appl. Earth Observ. Remote Sens.*, vol. 3, no. 4, pp. 576–593, Dec. 2010.
- [12] A. J. Luckman, "The effects of topography on mechanism of radar backscatter from coniferous forest and upland pasture," *IEEE Trans. Geosci. Remote Sens.*, vol. 36, no. 5, pp. 1830–1834, Sep. 1998.
- [13] J. T. Pulliainen, L. Kurvonen, and M. T. Hallikainen, "Multitemporal behavior of L- and C-band SAR observations of boreal forests," *IEEE Trans. Geosci. Remote Sens.*, vol. 37, no. 2, pp. 927–937, Mar. 1999.
- [14] M. Santoro, L. Eriksson, J. Askne, and C. Schmullius, "Assessment of stand-wise stem volume retrieval in boreal forest from JERS-1 L-band SAR backscatter," *Int. J. Remote Sens.*, vol. 27, no. 16, pp. 3425–3454, Aug. 2006.
- [15] A. Luckman, J. Baker, T. M. Kuplich, C. D. F. Yanasse, and A. C. Frery, "A study of the relationship between radar backscatter and regenerating tropical forest biomass for spaceborne SAR instruments," *Remote Sens. Environ.*, vol. 60, no. 1, pp. 1–13, Apr. 1997.
- [16] E. J. Rignot, J. Way, C. Williams, L. Viereck, and J. Yarie, "P-band radar mapping of forest biomass in boreal forests of interior Alaska," in *Proc. IEEE IGARSS*, Pasadena, CA, USA, 1994, vol. 3, pp. 1853–1855.
- [17] G. Sandberg, L. M. H. Ulander, J. E. S. Fransson, J. Holmgren, and T. L. Toan, "L- and P-band backscatter intensity for biomass retrieval in hemiboreal forest," *Remote Sens. Environ.*, vol. 115, no. 11, pp. 2874–2886, Nov. 2011.
- [18] S. Enghart, V. Keuck, and F. Siegert, "Aboveground biomass retrieval in tropical forests—The potential of combined X- and L-band SAR data use," *Remote Sens. Environ.*, vol. 115, no. 5, pp. 1260–1271, May 2011.
- [19] J. M. Kellendorfer, M. C. Dobson, J. D. Vona, and M. Clutter, "Toward precision forestry: Plot-level parameter retrieval for slash pine plantations with JPL AIRSAR," *IEEE Trans. Geosci. Remote Sens.*, vol. 41, no. 7, pp. 1571–1582, Jul. 2003.
- [20] K. J. Ranson, S. Saatchi, and G. Sun, "Boreal forest ecosystem characterization with SIR-C/XSAR," *IEEE Trans. Geosci. Remote Sens.*, vol. 33, no. 4, pp. 867–876, Jul. 1995.
- [21] T. Le Toan, S. Quegan, I. Woodward, M. Lomas, N. Delbart, and G. Picard, "Relating radar remote sensing of biomass to modelling of forest carbon budgets," *Clim. Change*, vol. 67, no. 2/3, pp. 379–402, Dec. 2004.
- [22] R. M. Lucas, A. K. Milne, N. Cronin, C. Witte, and R. Denham, "The potential of synthetic aperture radar (SAR) for quantifying the biomass of Australia's woodlands," *Rangeland J.*, vol. 22, no. 1, pp. 124–140, 2000.
- [23] S. Moreau and T. Le Toan, "Biomass quantification of Andean wetland forages using ERS satellite SAR data for optimizing livestock management," *Remote Sens. Environ.*, vol. 84, no. 4, pp. 477–492, Apr. 2003.
- [24] R. M. Lucas, N. Cronin, A. Lee, M. Moghaddam, C. Witte, and P. Tickle, "Empirical relationships between AIRSAR backscatter and LiDAR-derived forest biomass, Queensland, Australia," *Remote Sens. Environ.*, vol. 100, no. 3, pp. 407–425, Feb. 2006.
- [25] D. Lu, "The potential and challenge of remote sensing-based biomass estimation," *Int. J. Remote Sens.*, vol. 27, no. 7, pp. 1297–1328, Apr. 2006.
- [26] J. T. Pulliainen, P. J. Mikkela, M. T. Hallikainen, and J.-P. Ikonen, "Seasonal dynamics of C-band backscatter of boreal forests with applications to biomass and soil moisture estimation," *IEEE Trans. Geosci. Remote Sens.*, vol. 34, no. 3, pp. 758–770, May 1996.
- [27] E. P. W. Attema and F. T. Ulaby, "Vegetation modeled as a water cloud," *Radio Sci.*, vol. 13, no. 2, pp. 357–364, Mar./Apr. 1978.
- [28] M. Burgin, D. Clewley, R. Lucas, and M. Moghaddam, "A generalized radar backscattering model based on wave theory for multilayer multi-species vegetation," *IEEE Trans. Geosci. Remote Sens.*, vol. 49, no. 12, pp. 4832–4845, Dec. 2011.
- [29] R. Lucas, M. Moghaddam, and N. Cronin, "Microwave scattering from mixed-species forests, Queensland, Australia," *IEEE Trans. Geosci. Remote Sens.*, vol. 42, no. 10, pp. 2142–2159, Oct. 2004.
- [30] M. Neumann, S. S. Saatchi, L. M. H. Ulander, and J. E. S. Fransson, "Assessing performance of L- and P-band polarimetric interferometric SAR data in estimating boreal forest above-ground biomass," *IEEE Trans. Geosci. Remote Sens.*, vol. 50, no. 3, pp. 714–726, Mar. 2012.
- [31] A. C. Morel, S. S. Saatchi, Y. Malhi, N. J. Berry, L. Banin, D. Burslem, R. Nilus, and R. C. Ong, "Estimating aboveground biomass in forest and oil palm plantation in Sabah, Malaysian Borneo using ALOS PALSAR data," *Forest Ecol. Manage.*, vol. 262, no. 9, pp. 1786–1798, Nov. 2011.
- [32] T. Svoray, M. Shoshany, P. J. Curran, G. M. Foody, and A. Perevolotsky, "Relationship between green leaf biomass volumetric density and ERS-2 SAR backscatter of four vegetation formations in the semi-arid zone of Israel," *Int. J. Remote Sens.*, vol. 22, no. 8, pp. 1601–1607, May 2001.
- [33] J. N. Collins, L. B. Hutley, R. J. Williams, G. Boggs, D. Bell, and R. Bartolo, "Estimating landscape-scale vegetation carbon stocks using

- airborne multi-frequency polarimetric synthetic aperture radar (SAR) in the savannahs of north Australia," *Int. J. Remote Sens.*, vol. 30, no. 5, pp. 1141–1159, Jan. 2009.
- [34] J. R. Santos, M. S. P. Lacruz, L. S. Araujo, and M. Keil, "Savanna and tropical rainforest biomass estimation and spatialization using JERS-1 data," *Int. J. Remote Sens.*, vol. 23, no. 7, pp. 1217–1229, Apr. 2002.
- [35] E. T. A. Mitchard, S. S. Saatchi, I. H. Woodhouse, G. Nangendo, N. S. Ribeiro, M. Williams, C. M. Ryan, S. L. Lewis, T. R. Feldpausch, and P. Meir, "Using satellite radar backscatter to predict above-ground woody biomass: A consistent relationship across four different African landscapes," *Geophys. Res. Lett.*, vol. 36, no. 23, pp. L23401–1–L23401–6, Dec. 2009.
- [36] N. L. R. Cronin, "The potential of airborne polarimetric synthetic aperture radar data for quantifying and mapping the biomass and structural diversity of woodlands in semiarid Australia," Ph.D. dissertation, Univ. New South Wales, Sydney, Australia, 2004.
- [37] T. Castel, A. Beaudoin, N. Stach, N. Stussi, T. L. Toan, and P. Durand, "Sensitivity of space-borne SAR data to forest parameters over sloping terrain. Theory and experiment," *Int. J. Remote Sens.*, vol. 22, no. 12, pp. 2351–2376, Aug. 2001.
- [38] S. Tebaldini and F. Rocca, "Multibaseline polarimetric SAR tomography of a boreal forest at P- and L-bands," *IEEE Trans. Geosci. Remote Sens.*, vol. 50, no. 1, pp. 232–246, Jan. 2012.
- [39] G. Montero, R. Ruiz-Peinado, and M. Muñoz, *Produccion de Biomassas y Fijacion de CO2 por los bisques Españoles*. Madrid, Spain: Ministerio de Ciencia y Tecnologia, 2005.
- [40] W. H. Burrows, M. B. Hoffman, J. F. Compton, and P. V. Back, "Allometric Relationships and Community Biomass Stocks in White Cypress Pine (*Callitris glaucophylla*) and Associated Eucalypts of the Carnarvon Area, Central Queensland," Australian Greenhouse Office, Canberra, Australia, 2001.
- [41] S. D. Hamilton, G. Brodie, and C. O'Dwyer, "Allometric relationships for estimating biomass in grey box (*Eucalyptus microcarpa*)," *Australian Forestry*, vol. 68, no. 4, pp. 267–273, Jan. 2005.
- [42] M. Shimada, O. Isoguchi, T. Tadono, and K. Isono, "PALSAR radiometric and geometric calibration," *IEEE Trans. Geosci. Remote Sens.*, vol. 47, no. 4, pp. 3915–3932, Dec. 2009.
- [43] L. Jong-Sen, "Digital image enhancement and noise filtering by use of local statistics," *IEEE Trans. Pattern Anal. Mach. Intell.*, vol. PAMI-2, no. 2, pp. 165–168, Mar. 1980.
- [44] O. Frey, M. Santoro, C. L. Werner, and U. Wegmüller, "DEM-based SAR pixel-area estimation for enhanced geocoding refinement and radiometric normalization," *IEEE Geosci. Remote Sens. Lett.*, vol. 10, no. 1, pp. 48–52, Jan. 2013.
- [45] U. Wegmüller, C. Werner, T. Strozzi, and A. Wiesmann, "Automated and precise image registration procedures," in *Analysis of Multi-Temporal Remote Sensing Images*, vol. 2, L. Bruzzone and P. Smits, Eds. Singapore: World Scientific, 2002, pp. 37–49.
- [46] M. A. Tanase, R. Panciera, K. Lowell, C. Aponte, J. M. Hacker, and J. P. Walker, "Forest biomass estimation at high spatial resolution: Radar versus lidar sensors," *IEEE Trans. Geosci. Remote Sens. Lett.*, vol. 10, no. 3, May 2014, to be published. [Online]. Available: <http://ieeexplore.ieee.org>
- [47] J. Askne, P. Dammert, J. Fransson, H. Israelsson, and L. M. H. Ulander, "Retrieval of forest parameters using intensity and repeat-pass interferometric SAR information," in *Proc. Retrieval Bio-Geophys. Parameters SAR Data Land Appl.*, Toulouse, France, 1995, pp. 119–129.
- [48] S. Saatchi, K. Halligan, D. G. Despain, and R. L. Crabtree, "Estimation of forest fuel load from radar remote sensing," *IEEE Trans. Geosci. Remote Sens.*, vol. 45, no. 6, pp. 1726–1740, Jun. 2007.
- [49] L. Breiman, "Random forests," *Mach. Learn.*, vol. 45, no. 1, pp. 5–32, Oct. 2001.
- [50] B. E. Boser, I. Guyon, and V. Vapnik, "A training algorithm for optimal margin classifiers," in *Proc. 5th Annu. Workshop Comput. Learn. Theory*, 1992, pp. 144–152.
- [51] J. J. van Zyl, "Unsupervised classification of scattering behavior using radar polarimetry data," *IEEE Trans. Geosci. Remote Sens.*, vol. 27, no. 1, pp. 36–45, Jan. 1989.
- [52] M. C. Dobson, F. T. Ulaby, L. E. Pierce, T. L. Sharik, K. M. Bergen, J. Kellendorfer, J. R. Kendra, Y. C. L. E. Li, A. Nashashibi, K. Sarabandi, and P. Siqueira, "Estimation of forest biophysical characteristics in Northern Michigan with SIR-C/X-SAR," *IEEE Trans. Geosci. Remote Sens.*, vol. 33, no. 4, pp. 877–895, Jul. 1995.
- [53] S. Saatchi, R. A. Houghton, A. Dos Santos, J. V. Soares, and Y. Yu, "Distribution of aboveground live biomass in the Amazon basin," *Global Change Biol.*, vol. 13, no. 4, pp. 816–837, Apr. 2007.
- [54] M. Santoro, C. Beer, O. Cartus, C. Schmullius, A. Shvidenko, I. McCallum, U. Wegmüller, and A. Wiesmann, "Retrieval of growing stock volume in boreal forest using hyper-temporal series of Envisat ASAR ScanSAR backscatter measurements," *Remote Sens. Environ.*, vol. 115, no. 2, pp. 490–507, Feb. 2011.

Mihai A. Tanase received the engineering diploma in forestry from Stefan cel Mare University, Suceava, Romania, in 1999, the diploma in economy from the Bucharest Academy of Economic Studies, Bucharest, Romania, in 2004, the M.Sc. degree in environmental management from the International Centre for Advanced Mediterranean Agronomic Studies, Paris, France, in 2007, and the Ph.D. degree in geography from the University of Zaragoza, Zaragoza, Spain, in 2010.

Since 2011, he holds a postdoctoral position at The University of Melbourne, Carlton, Australia, through the ARC Super Science Fellowship program. He is a Principal Investigator for ESA ERS, DLR TerraSAR-X, and ALOS-2 projects and participated in the K&C Initiative as a Coinvestigator. He is interested in the use of remote sensing for vegetation characterization. His current activity is focused on synthetic aperture radar (SAR), InSAR, and PolSAR data for fire severity estimation, vegetation recovery monitoring, and the retrieval of biogeophysical parameters of forests and agricultural crops.

Dr. Tanase was the recipient of the IEEE GRSS IGARSS Symposium Interactive Prize Paper Award in 2010.

Rocco Panciera received the Master degree in environmental engineering (hydrology) from the University of Trento, Trento, Italy, in 2003 and the Ph.D. degree in environmental engineering (remote sensing) from The University of Melbourne, Carlton, Australia, in 2010.

From 2009 to 2011, he was a Research Fellow at The University of Melbourne, working on algorithm development for NASA's Soil Moisture Active Passive mission. In 2011, he was the recipient of the Australian Research Council Super Science Fellowship for monitoring of key climate variables using synthetic aperture radar, and he is currently working in this role at the Cooperative Research Centre for Spatial information in Melbourne, Australia. His expertise and research interest encompass the use of active and passive microwave remote sensing observation for the estimation of near-surface soil moisture from space satellites. He has also designed and led several large-scale airborne experiments for satellite algorithm development, including the National Airborne Field Experiments and the Soil Moisture Active Passive Experiments.

Kim Lowell received the B.Sc. degree in forest management and the M.Sc. degree in forest biometrics from the University of Vermont, Burlington, VT, USA, and the Ph.D. degree in forest biometrics from Canterbury University, Christchurch, New Zealand.

Since completing his Ph.D. degree in forest biometrics, his research has been focused on quantitative and statistical analysis and modeling using geospatial technologies with emphasis on spatial statistics, geographic information systems, and remote sensing as applied to natural resources. He spent 20+ years as a professor at universities in the United States and (French) Canada where he accumulated extensive experience in teaching, research, and leadership of fundamental and applied research projects in quantitative analysis and modeling, and geospatial technologies. His research accomplishments include some 65 refereed scientific articles, 60 conference papers, 30+ graduate students that have completed their M.Sc. and Ph.D. degrees, and approximately \$5 million in grants won. From 1998 to 2000, he served as the Director for the Centre for Research in Geomatics at Laval University, Quebec City—an organization of some 20 senior academics and 100 graduate students, plus associated technical and support staff. He is currently with the Cooperative Research Centre for Spatial Information, The University of Melbourne, Carlton, Australia.

Siyuan Tian received the B.S. degree in earth information science and technology from the University of Geosciences, Wuhan, China, in 2011 and the M.S. degree in geomatics from The University of Melbourne, Carlton, Australia, in 2013.

In 2013, she worked on lidar/radar data fusion for forest biomass retrieval at the Cooperative Research Centre for Spatial Information, The University of Melbourne.

Ms. Tian is a student member of the IEEE Geoscience and Remote Sensing Society.

Alberto García-Martín received the B.S. degree in geography, the M.S. degree in geographic information system (GIS) and remote sensing, and the Ph.D. degree in geography and territorial planning from the University of Zaragoza, Zaragoza, Spain, in 2001, 2004, and 2009, respectively, where he is currently a Ph.D. student working in a research group (GEOFOREST) at the Department of Geography.

His research interests focus mainly on biomass estimation and postfire environmental response model through the integrated use of satellite remotely sensed data, field data, and GIS. In this context, he has worked on some national research projects, including LIGNOSTRUM, EROFUEGO, PIR-FIRE, and RS-FIRE.

Jeffrey P. Walker received the Bachelor's degrees in civil engineering and in surveying (with honors and university medal) and the Ph.D. degree in water resources engineering from the University of Newcastle, Callaghan, Australia, in 1995 and 1999, respectively.

His Ph.D. thesis was among the early pioneering research on the estimation of root-zone soil moisture from the assimilation of remotely sensed surface soil moisture observations. In 1999, he joined the NASA Goddard Space Flight Center to implement his soil moisture work globally. In 2001, he was with the Department of Civil and Environmental Engineering, The University of Melbourne, Carlton, Australia, as a Lecturer, where he continued his soil moisture work, including the development of the only Australian airborne capability for simulating new satellite missions for soil moisture. In 2010, he was appointed as Professor in the Department of Civil Engineering, Monash University, Clayton, Australia, where he is continuing this research. He is contributing to soil moisture satellite missions at NASA, ESA, and JAXA as a Science Definition Team member for the Soil Moisture Active Passive mission and a calibration/validation Team member for the Soil Moisture and Ocean Salinity and the Global Change Observation Mission—Water, respectively.